Attached Inflatable Decelerator (AID) Performance Evaluation and Mission-Application Study

HERMAN L. BOHON* AND ROBERT MISERENTINO†
NASA Langley Research Center, Hampton, Va.

Planetary-mission studies of entry into low-density atmospheres such as that of Mars have demonstrated the need for efficient deceleration at supersonic speeds and have prompted a research program to develop and evaluate an Attached Inflatable Decelerator (AID). Wind-tunnel models were successfully deployed at supersonic speeds in less than 0.6 sec without excessive shock loads. The models were very stable throughout the Mach-number range from 2.0–4.75 and at angles of attack through 10° and had a high drag coefficient (1.14). The test data indicated that the permeability of the canopy rear surface is a primary factor in obtaining good drag performance. A mission study demonstrated the advantage of the AID as the first stage of a two-stage deceleration system for entry into the low-density atmosphere of Mars. The AID relaxes stringent deployment conditions on the terminal parachute; but the significant advantage is the large increases in landed-payload mass without increasing the size of the basic entry aeroshell.

Nomenclature

A = frontal area
B_E = entry-ballistic coefficient, $m_t/(C_DA)_e$
C_D = drag coefficient based on frontal area
C_m = pitching-moment coefficient
C_N = nomal-force coefficient
C_v = inlet-discharge coefficient
D = total diameter of AID (see Fig. 2)
D_o = norminal diameter of parachute
F_A = axial force
M = freestream Mach number
m = mass
P = air permeability at 0.5-in. H_2O pressure
p,q = static and dynamic pressure
t = time
α = angle of attack
$(C_DA)_d$ = drag area of entry body and inflated AID
$(C_DA)_e$ = drag area of entry body

Subscripts

b = base
e = entry
i = internal
t = total
∞ = freestream

Introduction

ATTEMPTS to extend the application of large parachutes to Mach numbers greater than 2 have revealed stability problems[1] which may seriously decrease the drag coefficient of the parachute in a supersonic environment. Small drogue parachutes, for example, have been employed at high supersonic speeds for stabilization and deceleration of small projectiles; however, the high values of geometric porosity required to obtain good stability characteristics have resulted in low drag coefficients.[2]

The need for efficient deceleration at high supersonic speeds has prompted a research program to develop and evaluate an Attached Inflatable Decelerator (AID), a low mass, inflatable canopy attached directly to a payload.[3] The concept is illustrated in Fig. 1, in which the canopy is shown attached to a conical planetary entry aeroshell.

The analytical development of AID configurations is presented in Ref. 3 and data from supersonic wind-tunnel tests of AID models deployed by using a liquid-vaporization system are presented in Ref. 4. Liquid-vaporization systems may be cumbersome in very large models; therefore, other methods of canopy deployment may be desired. In the present paper, the results of an experimental program to evaluate deployment and performance characteristics of AID models with a ram-air deployment system are presented (see Fig. 1).

Also presented is the evaluation of an AID in a typical Mars planetary-entry mission. Evaluation is based on performance characteristics of the supersonic wind-tunnel data presented herein and a decelerator mass optimization procedure.[5] Entry trajectories for the Mars 1970 minimum scale height atmosphere are utilized to determine optimum deployment conditions for a two-stage deceleration system consisting of an AID deployed at high supersonic speeds and a parachute deployed at transonic speeds.

Model Description

The AID configuration utilizes many load-carrying meridional tapes overlaying a lightweight coated fabric as shown in Fig. 1. Ram-air inlets at the periphery of the aeroshell initiate canopy deployment from its packaged mode. The ram-air inlets forward of the burble fence complete the inflation process and maintain the canopy internal pressure. The number and the size of the inlets were determined by the canopy volume to be inflated and the desired deployment rate.

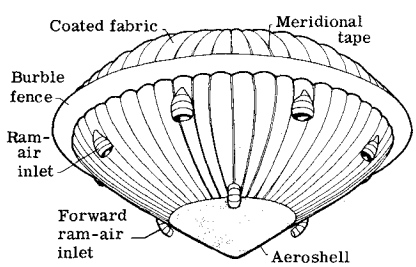

Fig. 1 Attached inflatable decelerator (AID).

Presented as Paper 70-1163 at the AIAA Aerodynamic Deceleration Systems Conference, Dayton, Ohio, September 14–16, 1970; submitted September 21, 1970; revision received April 15, 1971.

* Head, Aerothermoelasticity Section, Structures Division. Member AIAA.
† Aerospace Engineering. Member AIAA.

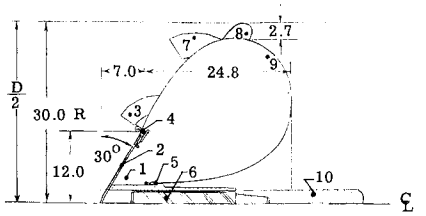

1 Decelerator stowage compartment
2 Aeroshell
3 Forward ram-air inlet
4 Forward attachment clamp
5 Rear attachment clamp
6 Six-component balance
7 Ram-air inlet
8 Burble fence
9 Inflatable decelerator
10 Sting support

Fig. 2 Supersonic AID configuration; all dimensions are in inches.

Four models were constructed for the present tests. Details of a typical model are shown in Fig. 2. The AID models have a frontal diameter D of 60 in. and are attached to an aluminum 120° conical aeroshell 24 in. diam. For the wind-tunnel tests, the aeroshell was rigidly attached to a support sleeve which mated with a six-component balance. The AID models were constructed from 1.86 ozm/yd² nomex fabric coated with 0.5 ozm/yd² viton. All models had four ram-air inlets 2.5 in. in diam. at the edge of the aeroshell and one model had an additional set of four ram-air inlets 4 in. in diameter in front of the burble fence. Fabrication details of the models, excluding the aeroshell inlets, are presented in Ref. 6.

Supersonic Wind-Tunnel Tests

The models were tested at the Arnold Engineering Development Center in the 16-ft propulsion wind tunnel. Some of the preliminary test data are presented in Ref. 7. The model test setup is shown in Fig. 3 and a photograph of the packaged model in the test section is shown in Fig. 4. The canopy was packaged in the base of the aeroshell and held in place with a daisy-chain arrangement consisting of small loops of tape attached to the meridional tapes (see Fig. 4.) The daisy chain was released by severing a single restraining cord with a pyrotechnic cutter. The aeroshell inlets were held in place by cords as shown in Fig. 4 which were severed in two locations to permit symmetrical deployment of the inlets. Torsion springs attached to the aeroshell at the periphery forced the inlets into the airstream.

All four models were successfully deployed in the supersonic stream; model designations and AID deployment conditions are given in Table 1. Model 1 had eight inlets, four at the aeroshell periphery and four rear inlets at the burble fence. All other models had four inlets, all at the aeroshell periphery. Model 3 was a refurbished model 2; that is, two canopy gores were replaced after the test on model 2 and the canopy was retested as model 3.

Deployment Performance and Inlet Efficiency

Deployment characteristics

A typical deployment sequence of the AID obtained from motion picture film is shown for model 2 in Fig. 5. The time $t = 0$ corresponds to the aeroshell inlets first facing the airstream. The rapid deployment of the canopy caused some momentary hang-up of the daisy chains of models 1, 2, and 3 and resulted in unsymmetrical deployment. Model 4 deployed uniformly but required the longest inflation time due to the loss of flow through the perforated fabric surface.

Table 1 Aid deployment conditions

Model	No. inlets	P, ft³/min-ft²	Mach number, M	q_∞, lbf/ft²	P_∞, lbf/in.²
1	8	0.02	3.0	120	19.1
2, 3, 4	4	0.02, 0.02, 10	4.4	73	5.5

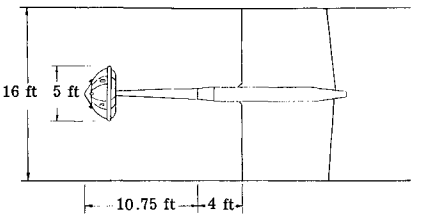

Fig. 3 AID model deployment test setup.

The variations of axial force and canopy internal-pressure ratio during deployment are shown in Figs. 6a-d. At time $t = 0$ the front inlets were facing the stream and the axial load was that on the aeroshell prior to deployment. The major axial-force disturbance during deployment occurred in all tests at about 0.1 sec when the rearward movement of the canopy ceased. This shock load was normally small in magnitude and was never greater than the total drag load.

Ram-air inlet efficiency

The method of inflating the test models provides an opportunity for realistic evaluation of the orifice discharge coefficient of the cloth inlets by correlation of the measured inflation rate with theoretical predictions. Air was assumed to flow into the canopy of constant volume through inlets and out of the canopy through the porous fabric. Isentropic-flow equations[8] for flow through an orifice have been adapted to the flow regimes of the model.

The discharge coefficient C_w was determined by using the internal-pressure history for model 2 since the deployment was fairly uniform and involved only aeroshell inlets. The permeability P of the surface is dependent on the pressure ratio across the canopy and on the magnitude of the internal pressure. Only the permeability of the rear surface was considered since the pressure across this surface was much greater than that of the front surface. The variation of permeability with pressure was measured on canopies of the wind-tunnel design, and the results are presented in Ref. 9. The canopy filling rate was calculated by using a discharge coefficient which resulted in the best comparison with the experimental pressure history for model 2. The resulting discharge coefficient is shown in Fig. 7a and the corresponding correlation of pressure history for model 2 is shown in Fig. 7b. The discharge coefficient for sharp-edged orifices[8] is shown by the dashed curve. This same variation with pressure ratio was used for the cloth inlets, however, the magnitude of the pressure ratio is only 70% of that for the sharp-edged orifice.

During initial unfurling of the canopy from the packaged mode ($0 < t < 0.15$ sec) the average pressure ratio p_i/p_t across the inlet was about 0.4; thus, for p_i/p_t less than 0.4 the discharge coefficient was assumed to be constant, as indicated by

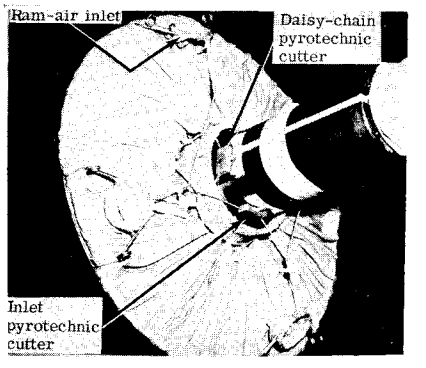

Fig. 5 Photographs of the AID deployment sequence; model 2, $M = 4.4$, $q_\infty = 73$ lbf/ft².

the solid horizontal curve in Fig. 7a. No attempt was made to correlate the pressure history during this time interval, but as can be seen from Fig. 7b, the pressure history from 0.15 sec–0.7 sec is closely predicted.

The discharge coefficient obtained from data for model 2 was used to calculate filling rates of the other three models; the results are shown in Fig. 8. The experimental pressure variations shown by the solid curves are obtained from Figs. 6a, c, and d. For model 1 (Fig. 8a) the rear inlets were assumed to contribute to the filling rate after 0.17 sec. The effect of the four rear inlets is to significantly increase the filling rate. The discharge coefficient used for the front inlets was also used for the rear inlets. The initial permeability of model 4 is much greater than that of the other three models, and the variation of P with internal pressure has not been determined experimentally. Thus, for model 4 a permeability variation with internal pressure was chosen which resulted in an equilibrium model pressure closely matching the maximum recovery pressure of model 4. All of the calculations are seen to be in reasonable agreement with the experimental results and lend credence to the value of discharge coefficient determined for cloth-type ram-air inlets.

Steady-State Performance

Variation of C_m, C_N, and C_D with α.

After deployment of the AID models, the pitching-moment and normal-force coefficients were determined for the four models through 10° angle of attack (see Fig. 9). The pitching-moment coefficient is based on the total frontal diameter of 60 in.

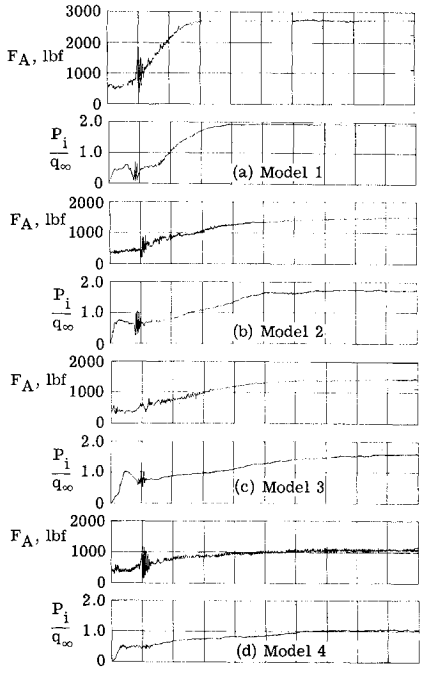

Fig. 6 Variation of axial force and internal-pressure ratio during deployment of models 1–4 (see Table 1).

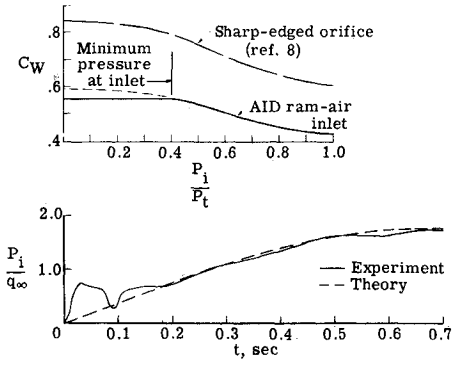

Fig. 7 Discharge coefficient and pressure histories for model 2.

The variation of drag coefficient with angle of attack is shown in Fig. 10 for model 1 prior to AID deployment (120° aeroshell) and after deployment. Study of the motion picture film indicates the plane of the burble fence remains normal to the direction of flow; consequently, there is little degradation in C_D with angle of attack.

Ram-air pressure recovery

The canopy internal pressure obtained from ram air is shown in Fig. 11 as a function of freestream Mach number. The test results illustrate the effect of inlet location and cloth permeability on recovery pressure. The circle symbol at Mach 3 is the pressure recovered with the dual inlets of model 1. A tunnel malfunction causing loss of flow destroyed the model shortly after deployment and data at other Mach numbers were not obtained. The solid line from Ref. 4 is the recovery pressure obtained from models with inlets at the burble fence only and shows good agreement with the test point from model 1. In the absence of the inlets at the burble fence, models 2 and 3 show a lower recovery pressure over the Mach-number range from 2–4.75. The variation of the pressure ratio with Mach number is similar to that obtained in Ref. 4.

The pressure recovered with the perforated model 4 is only 53% of that of model 1 and 60% of that of models 2 and 3. The result of the low internal pressure is a canopy profile less blunt than the design shape. Although the entire canopy of model 4 was perforated uniformly to increase the cloth permeability by over two orders of magnitude more than that of the other models, the major flow loss appears to be over the rear surface where the pressure difference between the interior and exterior surfaces of the canopy is sufficiently high to cause flow to escape at sonic velocity. The pressure difference across a major portion of the front surface is very low. Consequently, flow loss through the front surface is at low subsonic

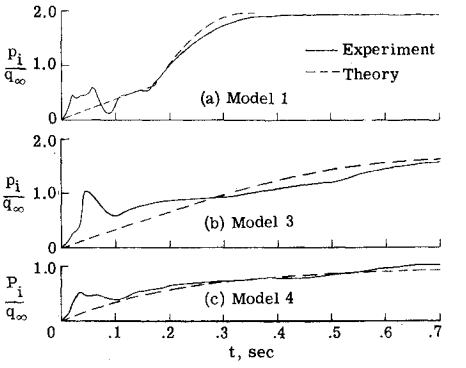

Fig. 8 Comparison of experimental and theoretical filling times.

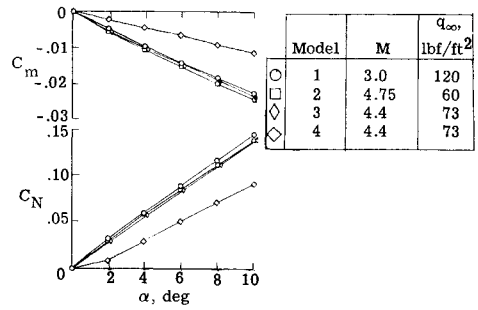

Fig. 9 Variation of pitching-moment and normal-force coefficients with angle of attack.

speeds and may have negligible effect on the AID performance.

Drag performance

The over-all drag characteristics of the AID models in the supersonic stream are shown in Fig. 12 where the drag coefficient from all models is plotted as a function of Mach number. The pressure recovery is seen to have a pronounced effect on the drag performance. The high-pressure recovery of model 1 resulted in a good drag coefficient of 1.14 at Mach 3 which is essentially the value predicted by the theory of Ref. 3 for the design shape. The solid curve from Ref. 4 is the drag coefficient obtained for similar models with the same pressure recovery as that of model 1. The lower pressure recovered with models 2 and 3 (see Fig. 11) resulted in a 10% reduction in C_D, and model 4 had a drag coefficient of only 61% of that of model 1. The drag coefficient in all cases is based on the design base diameter D (see Fig. 2). As was the case with ram-air pressure, the variation of C_D with Mach number is small. Thus, while low permeability of the rear canopy is essential to good drag performance of an AID, the permeability of the front surface is much less critical.

Mission Application

Two-Stage Deceleration System

The experimental data obtained herein have demonstrated that the AID can be deployed rapidly with ram air, has good static stability, and has good aerodynamic performance characteristics in the supersonic speed range independent of Mach number and dynamic pressure. The utility of the AID is best seen when applied to a planetary-entry mission into a low-density atmosphere such as that postulated for Mars. To illustrate the advantages of the AID in such a Mars mission, a tradeoff study has been configured around a two-stage deceleration system consisting of an AID and a subsonic parachute.

The rationale of a two-stage deceleration system is evident from Fig. 13 where the drag coefficients of the AID and of disk-gap-band and ringsail parachute are shown as functions of Mach number. The AID has a high drag coefficient in the supersonic range which is reduced considerably in the subsonic range. On the other hand, the subsonic parachutes are

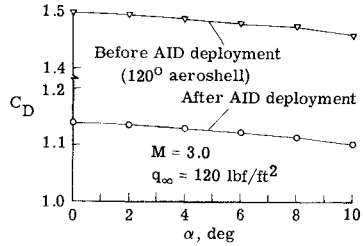

Fig. 10 Variation of drag coefficient for model 1 with angle of attack.

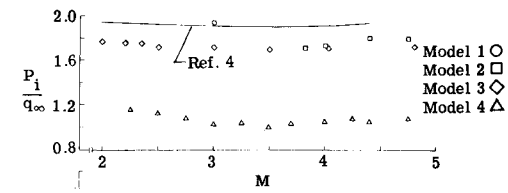

Fig. 11 Variation of ram-air pressure with Mach number.

very effective at subsonic speeds but experience a rapid loss in drag coefficient at Mach numbers above about 1.5. Thus, application of the parachute at $2 \leq M \leq 2.5$ would be inefficient at best and their use above $M = 2.5$ is beyond the state of the art. Therefore, the two-stage system studied utilized an AID deployed at supersonic speeds to decelerate to $M = 1.5$; a subsonic parachute was then deployed for terminal deceleration.

Trajectory Calculations

Trajectory calculations were performed using the Mars 1970 minimum scale height atmosphere. Results of these calculations are presented in Fig. 14 where the drag-area ratio $(C_DA)_d/(C_DA)_e$ is plotted as a function of Mach number at deployment. A sample trajectory is shown by the insert in Fig. 14. Entry is made from an altitude of 800,000 ft, at an inertial velocity of 15,000 ft/sec, and at a flight-path angle of

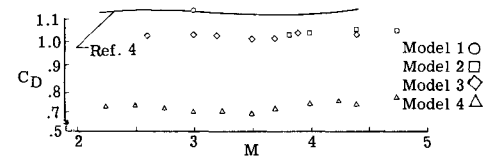

Fig. 12 Variation of drag coefficient with Mach number.

$-18°$. The entry trajectory in the insert is for an aeroshell ballistic coefficient, $B_E = 0.5$ slug/ft² and shows impact at supersonic speed. By deploying a decelerator to increase the C_DA ratio, the trajectory is altered as shown and the entry mass is decelerated to $M = 1.5$ at an altitude of 12,000 ft. A subsonic parachute then deployed must decelerate the remaining mass to a retrofire condition corresponding to a relative velocity of 300 ft/sec at an altitude of 6000 ft and a flight-path angle between $-60°$ and $-90°$. The curves shown in Fig. 14 for the four ballistic numbers give the combinations of drag-area ratio and deployment Mach number which meet the prescribed goal at $M = 1.5$. Solid marks representing deployment dynamic pressure are shown on the curves.

Mass Calculations

The dynamic pressure at parachute deployment ($M = 1.5$) is low and the parachute will nearly always be fabricated from minimum gage material. However, for the supersonic decelerator, many combinations of drag area and deployment conditions will meet the prescribed goal at $M = 1.5$; therefore, an optimization procedure, described in Ref. 5, is applied

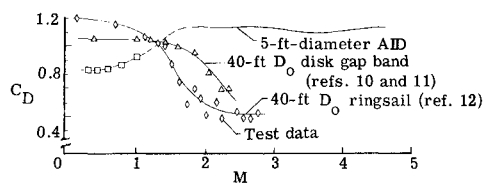

Fig. 13 AID and parachute drag performance.

Table 2 Optimized decelerator mass for Mars mission in 1970 minimum scale height atmosphere; entry vehicle: 11.5 ft-diam, 140° conical aeroshell

System variable	Deceleration system					
	Parachute		AID + parachute			
$m_t/(C_DA)_e$, slugs/ft²	0.32	0.4	0.32	0.4	0.5	0.6
Entry mass, lbm	1720	2150	1720	2150	2690	3220
Aeroshell + ablator, lbm	175	185	175	185	196	205
Residual mass, lbm	1304	1712	1304	1712	2226	2731
Deployment conditions:						
AID q_∞, lbf/ft²			18	47	75	86
AID M			2.3	4.1	5.0	5.0
Parachute q_∞, lbf/ft²	17	23.6	8.5	8.5	8.5	8.5
Parachute M	2.3	2.5	1.5	1.5	1.5	1.5
Decelerator size, ft:						
AID, D			18	21	26	41
Parachute, D_o	55	61.5	55	61.5	68.8	75.5
Decelerator mass, lbm:						
AID			18	32	78	300
Parachute	69	120	42	57	76	96
Total decelerator mass, lbm	69	120	60	89	154	396
Retropropulsion mass, lbm	110	138	110	138	172	206
Landed-payload mass, lbm	1125	1454	1134	1485	1900	2129

to the data in Fig. 14 to determine the drag-area ratio and deployment dynamic pressure at which the AID will have minimum mass. The mass equations for both the AID and the subsonic parachute are also given in Ref. 5. Detailed results of the tradeoff study are given in Table 2. The landed-payload mass is determined for the case of deceleration by parachute only and for the two-stage system. The entry body is an 11.5-ft-diam, 140° conical aeroshell and the increase in entry mass is a direct increase in ballistic number. The residual mass excludes the mass of the aeroshell and the ablator plus contingencies such as guidance controls, power supply, and harnesses which are separated at parachute deployment. The variation of aeroshell and ablator mass with B_E is obtained from Ref. 13 and the contingency mass and retropropulsion mass are provided from studies by the Viking Project Office at the Langley Research Center.

For $B_E = 0.32$ slug/ft² deployment conditions for the single-stage parachute are $M = 2.3$ and $q_\infty = 17$ lbf/ft², whereas parachute deployment conditions for the two-stage system are relaxed to $M = 1.5$ and $q_\infty = 8.5$ lbf/ft² for all values of B_E. the primary advantage of the AID is realized at higher values of B_E which show significant gains in landed-payload mass, as is apparent in Fig. 15. The landed-payload mass shown by the upper curve corresponds to that portion of the entry mass which touches down on the Mars surface. Supersonic deceleration at high Mach numbers may cause severe aerodynamic heating of the decelerator. The Mach number at which thermal protection would be required for an AID in a Mars atmosphere has not been established. In order to be assured of acceptable temperature levels on the decelerator fabric a design constraint of $M \leq 5$ was used for the AID. Without this constraint on Mach number, the decelerator mass and landed-payload mass would be that shown by the dashed curves. For $B_E = 0.32$ slug/ft² the landed-payload mass is 1134 lbm. Use of the two-stage deceleration system permits large increases in entry-ballistic coefficient which results in sizable gains in landed payload. Increasing the entry mass 1500 lbm to $B_E = 0.6$ results in a 995-lbm increase in landed payload. This gain is achieved without increasing the size of the basic entry aeroshell.

Conclusion

Four wind-tunnel models were successfully deployed at supersonic speeds. One model was deployed at Mach 3 and three models were deployed at Mach 4.4. Deployments occurred very rapidly (less than 0.6 sec) without excessive shock loads. The models were very stable throughout the Mach-number range from 2.0–4.75 and at angles of attack through 10°.

The advantage of the AID is demonstrated in the application as the first stage of a two-stage deceleration system for planetary entry into the low-density atmosphere of Mars. The calculations indicated the AID relaxes stringent deploy-

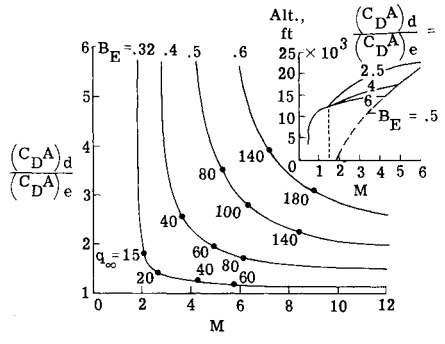

Fig. 14 Decelerator area required to achieve conditions of $M = 1.5$ at altitude of 12,000 ft in Mars 1970 minimum scale height atmosphere, entry velocity = 15,000 ft/sec.

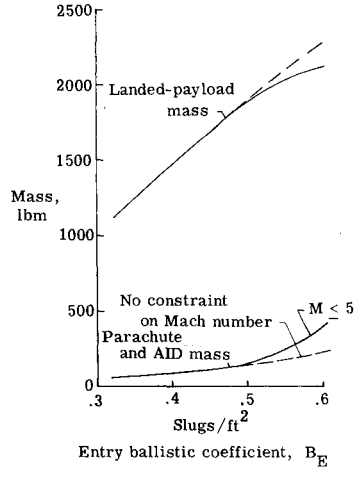

Fig. 15 Variation in decelerator mass and landed-payload mass with ballistic coefficient for two-stage decelerator system in Mars 1970 minimum scale height atmosphere.

ment conditions on the terminal parachute even for a ballistic coefficient of 0.32 slug/ft^2; but the significant advantage is the large increases in landed-payload mass made possible with the AID without increasing the size of the basic entry aeroshell.

References

[1] Gillis, C. L., "Aerodynamic Deceleration Systems for Space Missions," AIAA Paper 68-1081, Philadelphia, Pa., 1968.

[2] Alexander, W. C. and Lau, R. A., "State-of-the-Art Study for High-Speed Deceleration and Stabilization Devices," CR-66141, 1966, NASA.

[3] Mikulas, M. M., Jr. and Bohon, H. L., "Development Status of Attached Inflatable Decelerators," *Journal of Spacecraft and Rockets*, Vol. 6, No. 6, June 1969, pp. 654–660.

[4] Bohon, H. L. and Miserentino, R., "Deployment and Performance Characteristics of Five-Foot (1.5 m) Diameter Attached Inflatable Decelerators From Mach Number 2.2 to 4.4," TN D-5840, 1970, NASA.

[5] Anderson, M. S., Bohon, H. L., and Mikulas, M. M., Jr., "A Structural Merit Function for Aerodynamic Decelerators," TN D-5535, 1969, NASA.

[6] Barton, R. R., "Development of Attached Inflatable Decelerators for Supersonic Application," CR-66613, 1968, NASA.

[7] Baker, D. C., "Investigation of an Attached Inflatable Decelerator With Mechanically Deployed Inlets at Mach Numbers From 2.25 to 4.75," AEDC-TR-69-132, U.S. Air Force, June 1969, Arnold Engineering Development Center.

[8] Shapiro, A. H., "The Dynamics and Thermodynamics of Compressible Fluid Flow," Vol. I, Ronald Press, 1953, pp. 83–100.

[9] Deaton, J. W. and Willis, C. M., "The Effects of Uniaxial and Biaxial Tensile Loads and Load Cycling on the Air Permeability of a Lightweight Coated Fabric," AIAA Paper 70-1178, Dayton, Ohio, 1970.

[10] Preisser, J. S. and Eckstrom, C. V., "Flight Test of a 40-Foot-Nominal-Diameter Disk-Gap-Band Parachute Deployed at a Mach Number of 0.91 and a Dynamic Pressure of 11.6 Pounds Per Square Foot," TM X-1575, 1968, NASA.

[11] Eckstrom, C. V. and Preisser, J. S., "Flight Test of a 40-Foot-Nominal-Diameter Disk-Gap-Band Parachute Deployed at a Mach Number of 2.72 and a Dynamic Pressure of 9.7 Pounds Per Square Foot," TM X-1623, 1968, NASA.

[12] Eckstrom, C. V., "High Altitude Flight Test of a 40-Foot-Diameter (12.2 m) Ring-Sail Parachute at a Deployment Mach Number of 2.95," TN D-5796, 1970, NASA.

[13] Guy, L. D., "Structural and Decelerator Design Options for Mars Entry," *Journal of Spacecraft and Rockets*, Vol. 6, No. 1, Jan. 1969, pp. 44–49.